Micropatterning of TiO2 Thin Film in an Aqueous Peroxotitanate Solution

ARTICLE *in* CHEMISTRY OF MATERIALS · FEBRUARY 2004

Impact Factor: 8.35 · DOI: 10.1021/cm030543i

Micropatterning of TiO_2 Thin Film in an Aqueous Peroxotitanate Solution

Yanfeng Gao, Yoshitake Masuda, and Kunihito Koumoto*

Department of Applied Chemistry, Graduate School of Engineering, Nagoya University, Furo-cho, Chikusa-ku, Nagoya 464-8603, Japan

Received August 28, 2003. Revised Manuscript Received January 13, 2004

We report micropatterning of TiO_2 thin film by a peroxotitanate complex deposition method, which was a method we developed recently. The deposition solution was obtained by dissolving titanic acid (H_2TiO_3) into a mixture solvent containing ammonia and hydrogen peroxide aqueous solution. The amorphous TiO_2 micropattern with a high resolution was achieved by using a template of photomodified self-assembled monolayers at room temperature. The film showed high purity, flatness, and crack-free characteristics. The fundamental dielectric characteristics suggest that the micropatterned TiO_2 thin films prepared by the present method are promising for application to dielectric layers.

Introduction

Site-selective fabrication of materials with micro-/nanofeatures in requisite areas is a bottom-up low-cost technique with good potential for application to biomedicine[1] and microelectronics.[2] Although production of small parts, now in the realm of nanoscopic dimensions, has been accomplished, integration into more complex structures and devices represents a major challenge. With evolution, however, nature has ingeniously succeeded in producing an impressive variety of inorganic functional structures with designed shape and size on specific sites through the biologically controlled biomineralization process, usually at near room temperature and in aqueous solutions.[3] Inspired by this process, micropatterning of thin films such as TiO_2,[4−6] ZrO_2,[7] $SrTiO_3$,[8,9] and SnO_2[10] has been achieved through chemical solution routes using the self-assembled monolayer (SAM) technique. This paper describes our progress in achieving site-selective deposition of crack-free TiO_2 thin films in an aqueous peroxotitanate solution at room temperature.

Titanium dioxide thin films have attracted both industrial and academic attention for such potential applications as a gate dielectric in metal oxide semiconductor field-effect transistors (MOSFETs),[11] a surface for solar energy conversion,[12] and high-efficiency photocatalysis[13] because of their well-known properties that include high refractive index, high permittivity, and transmittance in a visible region. To overcome some of the drawbacks of traditional methods, novel low-temperature processes for the one-step deposition of TiO_2 thin films have been developed through controlled hydrolysis of titanium species either with use of an organic solvent[6] or in an aqueous solution.[4,5,14,15] The hydrolysis of $(NH_4)_2TiF_6$,[4] $TiCl_4$,[14] or TiF_4[15] can yield either amorphous or crystalline TiO_2 thin films depending on the synthetic conditions employed. A complex peroxo precursor of titanium can also be employed for the deposition of TiO_2 thin films by several methods, such as electrochemical deposition[16a] and self-assembled monolayer technique.[16b] The peroxotitanium-type solution is usually prepared by adding droplets of pure $TiCl_4$ to an ice-cooled aqueous solution containing H_2O_2 with or without excess acid.[16] However, all of these methods use starting materials containing chlorine or fluorine, which would be present in the produced thin film, resulting in poor dielectric properties and environmental

* Corresponding author. E-mail: g44233a@nucc.cc.nagoya-u.ac.jp. Fax: +81-52-789-3201. Tel: +81-52-789-3327.

(1) (a) Chen, C. S.; Mrksich, M.; Huang, S.; Whitesides, G. M.; Ingber, D. E. *Science* **1997**, *276*, 1425. (b) Flemming, R. G.; Murphy, C. J.; Abrams, G. A.; Goodman, S. L.; Nealey, P. F. *Biomaterials* **1999**, *20*, 573. (c) Bai, J.; Snively, C. M.; Delgass, W. N. *Adv. Mater.* **2002**, *14*, 1546. (d) Ward, J. H.; Bashir, R.; Peppas, N. A. *J. Biomed. Mater. Res.* **2001**, *56*, 351.

(2) (a) Rogers, J. A.; Mirkin, C. *Mater. Res. Bull.* **2001**, *26*, 506. (b) Chou, S. Y.; Krauss, P. R.; Renstrom, P. J. *Science* **1996**, *272*, 85. (c) Chou, S. Y.; Keimel, C.; Gu, J. *Nature* **2002**, *417*, 835.

(3) (a) Bäuerlein, E. *Angew. Chem., Int. Ed.* **2003**, *42*, 614. (b) Mann, S. *Biomimetic Materials Chemistry*; VCH: New York, 1996; pp 1−40. (c) Aizenberg, J.; Muller, D. A.; Grazul, J. L.; Hamann, D. R. *Science* **2003**, *299*, 1205.

(4) Koumoto, K.; Seo, S.; Sugiyama, T.; Seo, W. S.; Dressick, W. J. *Chem. Mater.* **1999**, *11*, 2305.

(5) Collins, R. J.; Shin, H.; DeGure, M. R.; Heuer, A. H.; Shukenik, C. N. *Appl. Phys. Lett.* **1996**, *69*, 860.

(6) Bartz, M.; Terfort, A.; Knoll, W.; Tremel, W. *Chem.-Eur. J.* **2000**, *6*, 4149.

(7) Gao, Y.-F.; Masuda, Y.; Yonezawa, T.; Koumoto, K. *J. Ceram. Soc. Jpn.* **2002**, *110*, 379.

(8) Gao, Y.-F.; Masuda, Y.; Yonezawa, T.; Koumoto, K. *Chem. Mater.* **2002**, *14*, 5006.

(9) Gao, Y.-F.; Masuda, Y.; Koumoto, K. *Chem. Mater.* **2003**, *15*, 2399.

(10) Shirahata, N.; Masuda, Y.; Yonezawa, T.; Koumoto, K. *Langmuir* **2002**, *18*, 10379.

(11) Peercy, P. S. *Nature* **2000**, *406*, 1023.

(12) Bach, U.; Lupo, D.; Comte, P.; Moser, J. E.; Weissortel, E.; Salbeck, J.; Spreitzer, H.; Grätzel, M. *Nature* **1998**, *395*, 583.

(13) Linsebigler, A. L.; Guangquan, L.; Yates, J. T., Jr. *Chem. Rev.* **1995**, *95*, 735.

(14) Kim, K. J.; Benkstein, K. D.; Lagemaat, J. V. D.; Frank, A. J. *Chem. Mater.* **2002**, *14*, 1042.

(15) Shimizu, K.; Imai, H.; Hirashima, H.; Tsukuma, K. *Thin Solid Films* **1999**, *351*, 220.

(16) (a) Zhitomirsky, I.; Gal-Or, L.; Kohn, A.; Hennicke, H. W. *J. Mater. Sci.* **1995**, *30*, 5307. (b) Niesen, T. P.; Joachim, B.; Fritz, A. *Chem. Mater.* **2001**, *13*, 1552.

10.1021/cm030543i CCC: $27.50
Published on Web 02/20/2004

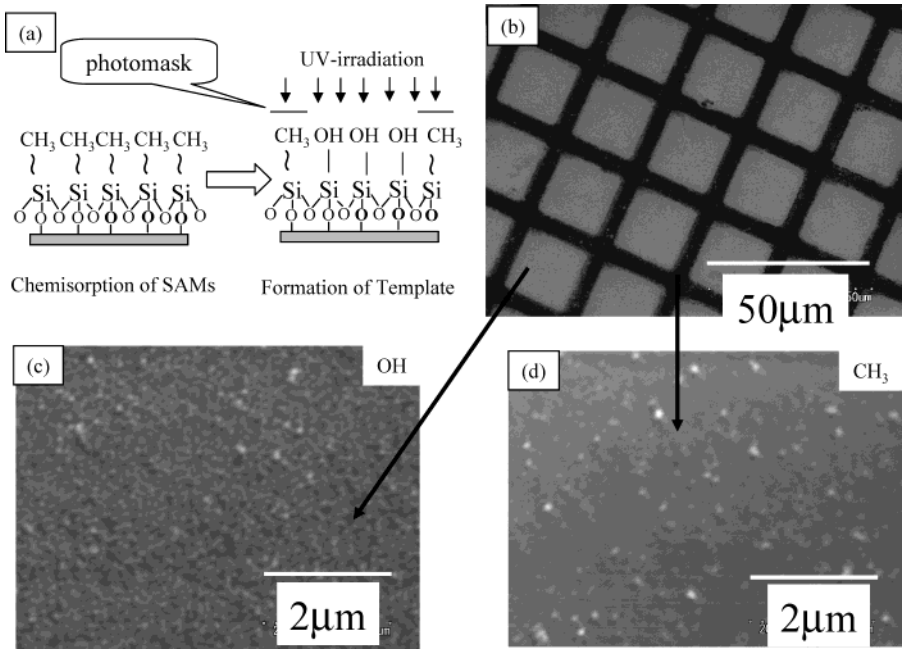

Figure 1. Schematic outline of the preparation of OTS self-assembled monolayers and region-selective modification by UV light (a); the as-deposited micropatterns of TiO_2 thin film prepared in a 5 mM aqueous peroxotitanate solution under pH 2.0 at 37 °C for 1 h (b); enlarged SEM photographs of silanol regions (c) and octadecyl regions (d).

concerns. Direct dissolution of TiO_2 into an aqueous solution avoids such problems.

We developed a novel solution system and succeeded in achieving direct deposition of a transparent, high-purity TiO_2 thin film in an aqueous peroxotitanate solution, which was prepared by dissolving metatitanic acid (H_2TiO_3) in a solvent mixture of concentrated H_2O_2 and $NH_3{\cdot}H_2O$.[17] Although various peroxotitanate species were formed at different pH levels, they remained stable long enough to allow the deposition of a thin film. The precipitate collected after deposition of TiO_2 thin film could be dissolved in the mixture of H_2O_2 and $NH_3{\cdot}H_2O$ aqueous solution and employed again for TiO_2 deposition. The present method is simple, inexpensive, and environmentally friendly, showing the potential for industrial application. However, issues such as the preparation of crack-free thin films and micropatterning must still be addressed.

Experimental Section

Sample Preparation through Peroxotitanate-Complex Deposition Process. The preparation of samples has been described in our previous paper.[17] Briefly, 3 g of H_2TiO_3 (80%, Mitsuwa) was added to an ice-cooled solvent consisting of 25 cm^3 of H_2O_2 (30% in H_2O, Mitsubishi) and 5 cm^3 of ammonia (25% in H_2O, Kishida). After the mixture was stirred for 90 min, a homogeneous pale yellow-green solution was obtained. This homogeneous solution was then diluted with deionized water (>18 MΩ cm) to 5 mM Ti^{4+} at pH 1.9−2.0 (adjusted by the addition of an appropriate amount of HNO_3). SAMs of octadecyl-trichloro-silane (OTS, Acros, New Jersey) were prepared on the p-Si substrate (Shinetsu; resistivity: 4−6 Ωcm) and UV modified by the method described in other papers.[4,7−10] The substrate was then floated on the surface of the diluted solution with the SAM surface upside down at room temperature (~24 or 37 °C) to deposit a thin film. After soaking for 1−120 h, the substrate was taken out of the solution, carefully rinsed with distilled water, and dried at 50 °C for 24 h. After deposition, the precipitate was also filtrated, rinsed with distilled water, and dried at 50 °C.

Characterization Techniques. A scanning electron microscope (SEM; model S-3000N, Hitachi) was used to observe the deposits on the substrate. A scanning probe microscope (SPI3800N, Seiko Instruments Inc.) was operated in AFM contact mode using a triangular-shaped Si_3N_4 cantilever to observe the topography of the films; scans were carried out at room temperature under ambient air with a frequency of 1−2 kHz. The structure and phase composition were characterized by X-ray diffraction (XRD; model RAD-1C, Rigaku; 40 kV, 30 mA) with Cu Kα radiation (λ = 0.15418 nm) at a scanning speed of 1°/min. The thickness and the refractive index of films were measured by a laser ellipsometer (PZ2000, Philips) with an incidence angle of 70° and wavelength of 632.8 nm. The zeta potential of the as-obtained powders was measured (ZETASIZER 3000HS_A, Malvern Instruments, U.K.) by dissolving a trace of powder in 50 mL of deionized water. The chemical composition of the deposited film was analyzed by X-ray photoelectron spectroscopy (XPS; Escalab210, VG Scientific Ltd.) with Mg Kα as the X-ray source operated at a constant pass energy of 18 eV. All spectra were referenced to the C_{1s} signal at 284.6 eV. Gold was evaporated onto both the as-deposited film (0.785×10^{-6} m^2) and the rear side of an Si wafer (approximately 1.225×10^{-5} m^2) to form electrodes for an MOS device. A source measurement unit (KEITHLEY236) and an impedance analyzer (HP4192A) were employed to measure the dielectric properties of the MOS device.

Results and Discussion

Micropatterning of TiO_2 Thin Film. SAMs possessing various functional groups have been employed to tailor the morphology of thin films or to control nucleation. SAMs themselves can be selectively modified by X-ray, electron/ion beam, and UV irradiation, producing an active surfactant with different physical and/or chemical properties.[9] Figure 1 shows a schematic outline of regio-selective surface modification of an octadecyltrichlorosilane (OTS)-SAM and micropatterning of TiO_2 thin films. UV irradiation through a photomask caused a photocleavage reaction on the exposed

(17) Gao, Y.-F.; Masuda, Y.; Peng, Z.; Yonezawa, T.; Koumoto, K. *J. Mater. Chem.* **2002**, *13*, 608.

areas, leaving unexposed areas unchanged. Hence, a template was formed, composed of the hydrophilic silanol region next to the hydrophobic octadecyl regions (Figure 1a). This surface could then be used as a template for fabrication of micropatterned thin films. Figure 1b shows the as-deposited TiO_2 thin films; the films were discrete TiO_2 areas of 20 × 20 μm^2 with intervals of 5 μm. The large contrast between octadecyl regions and silanol regions suggested successful selective deposition of TiO_2 film on the silanol regions. The selectivity was further confirmed on the basis of enlarged photographs of the silanol region (Figure 1c) and octadecyl region (Figure 1d); a dense film was formed on the silanol regions by coalescence of closely packed particles, compared to some fragmentary white grains that formed on the octadecyl regions. The resolution of the micropattern barely changed after cleaning by ultrasonication (150 W) for 2 min. The variation, 2.8%, was estimated by practical measurement of line widths and comparison to the line edge roughness, which is consistent with that of the photomask employed, indicating that a high resolution was obtained. Although further efforts must be made to miniaturize the dimensional features of our micropatterns considering the realization of nanosized devices, the present result is an inspiring first step toward a deeper understanding of solution−interface interaction and the self-assembly process.

Fabrication of colloid assemblies onto patterned SAMs that rely on either the electrostatic interaction between particles and surface or surfaces capillary forces have been reported.[18−20] Direct control over colloid self-assembly onto patterned SAMs offers several advantages over conventional methods, such as application of the external electric fields or manipulation of the interaction potential. Although the pK_a value of our as-deposited solid is not available due to its complex composition (discussed later in this paper), the practical measurement of the collected precipitate gave an isoelectric point at about 5.7 (result is not shown), which strongly suggests that the particles carry a positive charge under the present conditions (pH = 1.9). The silanol surface was positively charged or close to neutral at pH 1.9.[9] Hence, the electrostatic interaction plays a minor role and cannot explain the site-selective deposition on the silanol areas. In fact, the selective deposition of TiO_2 may be dominated by polar interactions, that is, chemical bond or hydrogen bond formation. In our case, even though the film was as thin as 19 nm, 100% coverage (observed by AFM) was still obtained by direct adsorption of reaction-produced colloid particles. Therefore, we deduce that repulsive interparticle interaction was not significant during deposition in this case.

Growth Rate, Refractive Index, and Roughness. Figure 2 shows the changes in film thickness, refractive index, and roughness with the deposition time. The

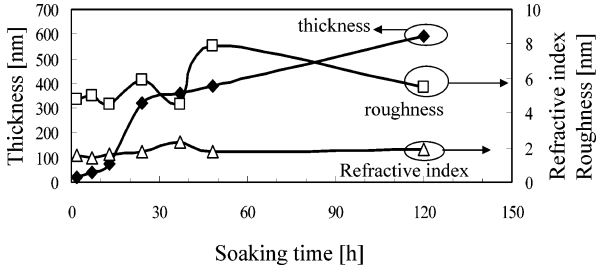

Figure 2. Relationship of film thickness, refractive index, and roughness dependent on the soaking time; the film was prepared in a 5 mM aqueous peroxotitanate solution under pH 2.0 at 24 °C.

thickness of the films with 100% coverage (confirmed by AFM) ranged from 19 to 590 nm, which could be easily controlled by deposition time (2−120 h). The change in the film thickness with time comprised three stages. During the initial 13 h, the film grew at a rate of 5−10 $nm \cdot h^{-1}$, which obviously increased to about 22 $nm \cdot h^{-1}$ during the period of 13−24 h. After 24 h, the film thickness continued to increase, whereas the growth rate significantly decreased to approximately 2−3 $nm \cdot h^{-1}$. The growth rate was closely related to the solution conditions and surface functions. The classical theory for nucleation and crystal growth indicates that the formation of particles begins with the generation of tiny nuclei in a supersaturated medium followed by growth. The latter process is controlled by mass transport and by the kinetics of the addition and removal of individual species such as atoms, ions, or molecules to and from the particle surfaces. Hereby, the driving force for the removal (dissolution) of those species increases with decreasing particle size. Thus, when there is a slight difference in the particle size, the large particles will grow at the expense of the smaller ones. This mechanism is called Ostwald ripening and is generally believed to be the major mechanism of crystal growth. Although it is difficult to clearly conclude whether the film was deposited by the surface-promoted heterogeneous nucleation or by the adsorption of particles generated through homogeneous nucleation to the surface in the very beginning of deposition, a certain induction period indeed exists, and hence the film growth rate in the initial stage was relatively low. With the reaction proceeding, the homogeneous nucleation dominated the formation of a solid phase and the solution became turbid. Film grew through the attachment of nuclei or clusters homogeneously formed in solution, resulting in a high growth rate. However, the solution became transparent again after about 24 h of soaking, suggesting that the film growth might have been governed by heterogeneous nucleation; that is growth through surface-promoted nucleation, resulting in a low growth rate. When a fresh substrate was immersed into a solution after aging for 13 h corresponding to the induction period shown in Figure 2, a similar change in growth rate was observed; a growth rate was high in the beginning, but it slowed after solution became transparent again. We therefore believe that the attachment of nuclei generated in the solution resulted in the accelerated growth rate we observed in the second period of time (13−24 h). In this stage, the supersaturation of the solution was much higher than that in the initial stage, which contributed to the higher

(18) (a) Zhu, P.-X.; Masuda, Y.; Koumoto, K. *J. Colloid Interface Sci.* **2001**, *243*, 31. (b) Krüger, C.; Jonas, U. *J. Colloid Interface Sci.* **2002**, *252*, 331. (c) Ye, Y.-H.; Badilescu, S.; Truong, V.-V.; Rochon, P.; Natansohn, A. *Appl. Phys. Lett.* **2001**, *79*, 872.

(19) (a) Aizenberg, J.; Braun, P. V.; Wiltzius, P. *Phys. Rev. Lett.* **2000**, *84*, 2997. (b) Demers, L. M.; Mirkin, C. A. *Angew. Chem., Int. Ed.* **2001**, *40*, 3069. (c) Lee, I.; Zheng, H.-P.; Rubner, M.-F.; Hammond, P. T. *Adv. Mater.* **2002**, *14*, 572.

(20) Tieke, B.; Fulda, K.-F.; Kampes, A. *Nano-surface Chemistry*; Rosoff, M., Ed.; Marcel-Dekker: New York, 2002; pp 213−242.

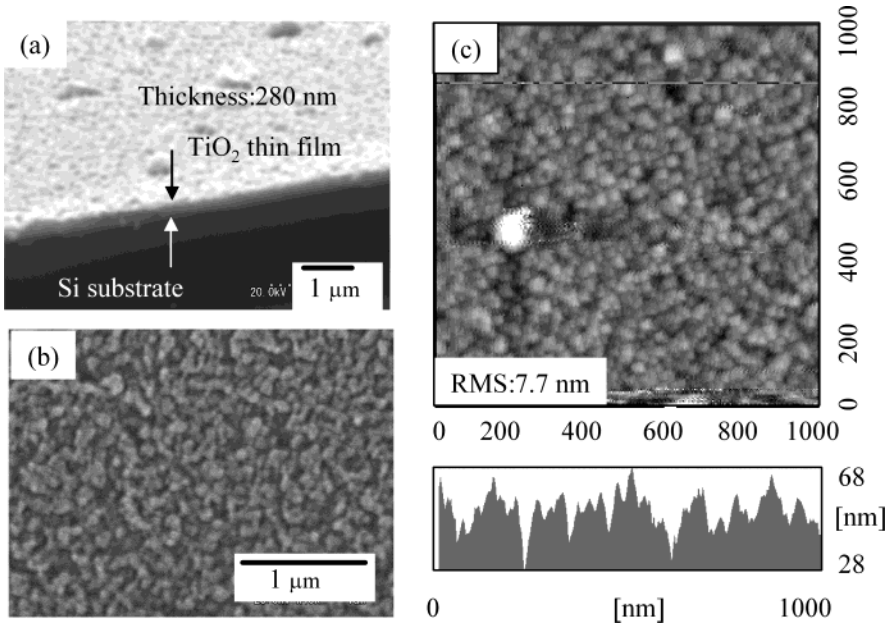

Figure 3. Cross-sectional SEM photograph (a), surface morphology (b), and topography (c) along with height profile along the corresponding line shown in the image for the TiO_2 thin film (corresponding thin film obtained after soaking for 24 h as shown in Figure 2) after annealing at 700 °C for 2 h in air.

growth rate and the large amount of precipitates accumulating at the bottom of the beaker. In the following stage, the growth rate decreased with the decreasing degree of supersaturation.

The surface morphologies of the as-deposited thin films were almost the same; the films were formed by coalescence of nanosized particles 10−20 nm in diameter, but the particles aggregated into large grains of 50−100 nm. The precipitates were preferential for filling the voids, resulting in the formation of a dense particulate film. All of the films demonstrated flat surfaces with root-mean-square (RMS) roughness of 5−8 nm for the measured areas of 500 × 500 nm^2 (Figure 2). However, the relative roughness (defined as RMS/thickness) obviously decreased with an increase in the film thickness, typically from 27% to 1%, by prolonging the soaking time from 2 to 120 h. The refractive index ranged from 1.5 to 1.8. Although the refractive index of the film increased with increasing soaking time, it is still low compared to that of the crystalline TiO_2 thin films (anatase: 2.3−2.54,[21] 2.75[21b]), which may be attributed to the amorphous characteristics and low density of the present as-deposited thin film.

Morphology and Topography of TiO_2 Thin Film after Annealing. The as-deposited thin film was amorphous, but it crystallized into anatase after annealing at a temperature as low as 300 °C (profiles are not shown). The energy needed for the phase transformation is relatively low, although we failed to achieve direct crystallization of thin films in the solution even after a series of attempts, including increasing the soaking temperature (from room temperature to 50 or 80 °C), changing the pH (2.0−7.0), and adding different anions (Cl^- or SO_4^{2-} from HCl or H_2SO_4, respectively). After annealing at 700 °C for 2 h in air (Figure 3), the film shrank from 306 to 280 nm in thickness (measured by both SEM and ellipsometer, Figure 3a), a shrinkage of 8.5%. The particle size observed by SEM (Figure 3b) and AFM increased slightly compared to that of the as-deposited one (data is not shown); however, no obvious cracks were observed in the SEM photograph (Figure 3b). The dark groove in the AFM image (Figure 3c) suggested the appearance of cracks, but the height profile showed that the deepest section (∼40 nm) was still much smaller than the film thickness (∼280 nm) (Figure 3a), suggesting that the cracks were superficial. Hence, we successfully deposited a virtually crack-free TiO_2 thin film with a thickness of 280 nm after annealing at 700 °C.

Chemical Composition. For determination of the chemical composition of the as-deposited amorphous thin film, XPS analysis was conducted (data is not shown). Only Ti, O, and C were present in the as-deposited thin film. No other elements, such as N, were detected. The carbon was presumably incorporated as a result of contamination during storage in air. Therefore, the as-deposited thin film was of high purity. The binding energies for $Ti_{2p3/2}$ were 458.8 eV. Peak separation of the O_{1s} spectrum clearly showed three kinds of oxygen with binding energies of 530.4, 532.3, and 533.6 eV, assigning to the Ti(IV)−O bonds,[22] OH groups,[23] and peroxo groups,[24] respectively. The quantitative analysis suggested a molar ratio of Ti/O = 1/2.4−1/2.6 for different samples, which was much lower than 1/2 for the stoichiometric TiO_2. The FT-IR result definitely confirmed the presence of Ti−O bond, peroxo groups, and OH groups.[17] These findings, along with those from

(21) (a) Zhang, J.-Y.; Boyd, I. W.; O'Sullivan, B. J.; Hurley, P. K.; Kelly, P. V.; Sénateur, J.-P. *J. Non-Cryst. Solids* **2002**, *303*, 134. (b) Martinu, L.; Poitras, D. *J. Vac. Sci. Technol. A* **2000**, *18*, 2619. (c) Wang, Z.-C.; Helmersson, U.; Käll, P.-O. *Thin Solid Films* **2002**, *405*, 50.

(22) Masuda, Y.; Jinbo, Y.; Yonezawa, T.; Koumoto, K. *Chem. Mater.* **2002**, *14*, 1236.

(23) Yu, J. C.; Zhang, L.-Z.; Zheng, Z.; Zhao, J.-C. *Chem. Mater.* **2003**, *15*, 2280.

(24) Rao, C. N. R.; Ganguly, P.; Hegde, M. S.; Sarma, D. D. *J. Am. Chem. Soc.* **1987**, *109*, 6893.

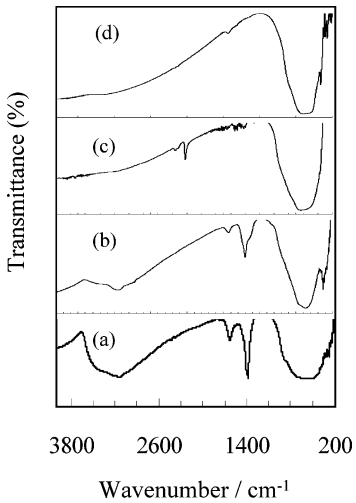

Figure 4. FT-IR spectra of the as-prepared powder (a) and those after annealing at different temperatures: (b) 200 °C; (c) 300 °C; (d) 400 °C.

XPS and TG-DTA, suggest a possible chemical composition of $TiO_{2-x-0.5y}(O_2)_x(OH)_y \cdot zH_2O$, which is similar to that deposited on a glass substrate.[17] After annealing at 700 °C, the molar ratio of Ti/O changed to 1/2.1, suggesting the decomposition of unstable groups such as OH and peroxo.

In the FT-IR spectrum (Figure 4) of the collected precipitate, a broad peak appearing at 3100−3600 cm^{-1} was assigned to fundamental stretching vibration of O−H hydroxyl groups (free or bonded),[25] which was further confirmed by a weak band at about 1620 cm^{-1}. The absorption band at 1620 cm^{-1} was caused by a bending vibration of coordinated H_2O as well as from Ti−OH. The bending vibrational mode of water may appear as shoulders on the spectrum at 3240 cm^{-1}. Peaks located at 500 and 430 cm^{-1} were likely due to the vibration of the Ti−O bonds in the TiO_2 lattice.[26] The peak centered at 900 cm^{-1} may be assigned to characteristic O−O stretching vibration,[26a] and the shoulder observed at 690 cm^{-1} may have been due to the vibration of the Ti−O−O bond. Although the peak detected at 1409 cm^{-1} could not be assigned, the FT-IR measurement firmly suggested the presence of Ti−O bonds, peroxo groups, and OH groups in the as-prepared precipitate.

After annealing at 200 °C (Figure 4b), the shoulder assigned to peroxo groups became weak, suggesting decomposition taking place. Peaks attributed to adsorbed water almost disappeared, while vibration of hydroxyl groups still could be observed at about 3140 cm^{-1}, which was not detected after annealing at 300 °C (Figure 4c). After annealing at 400 °C (Figure 4d), only peaks for Ti−O vibration located at 400−700 cm^{-1} were observed.

Dielectric Properties. The basic dielectric characteristics showed that the as-deposited thin film demonstrates typical capacitance−voltage (C−V, Figure 5a) and current−voltage properties (I−V, Figure 5b). For these measurements, a metal-oxide-semiconductor (MOS)

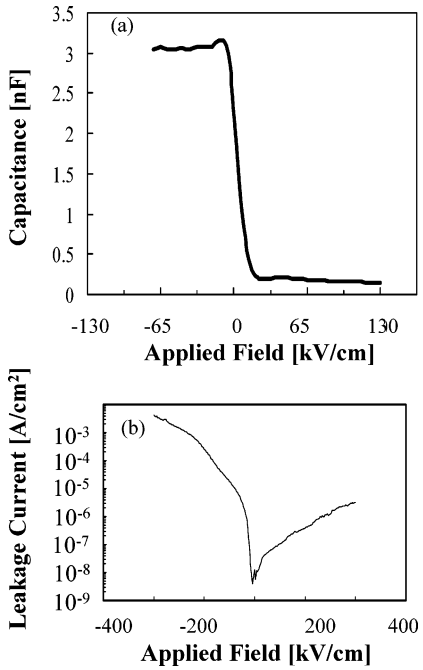

Figure 5. C−V and I−V characteristics of the as-deposited thin film; curves were obtained at room temperature.

capacitor ($Au/TiO_x/SiO_2/Si/Au$) was fabricated using Au as both top and bottom electrodes; this capacitor was formed by a parallel plate capacitor of TiO_2, SAM (about 2 nm according to the molecular structure of OTS), and an SiO_2 layer. The high-frequency (100 kHz) capacitance−voltage curve exhibited typical accumulation, depletion, and inversion areas as a result of the accumulation of major carriers (holes for p-type silicon) in the oxide−semiconductor interface or depletion of them when the bias was swept from a negative voltage to a positive one. The dielectric constant of 63 at 100 kHz for an as-deposited thin film (306 nm) was estimated by assuming the native silica layer to be 2 nm (the electrode area: 0.785 cm^2). Such a result is much larger than the reported value for biomimetically deposited amorphous TiO_2 (21.6,[27] 24−57[28]). This may be due to the specific composition of our thin film and/or existence of minor crystallized particles, although no crystalline phase was detected by XRD.

The leakage current (Figure 5b) at 1 V (∼35 kV/cm) was about 4.3×10^{-8} A cm^{-2}, which is relatively high considering the thickness of our as-deposited thin film (306 nm). The dielectric constant decreased almost linearly from 160 at 1 kHz to 23 at 1 MHz (bias voltage = −1 V), and the corresponding dispersion factor increased at above 100 kHz, reaching 0.9 at 1 MHz. All of these results may be associated with interface states and impurities such as OH^- and H_2O. The film surface, as clearly seen in Figure 3b, exhibits discrete particulate characteristics, which should have a significant effect on the leakage current. However, the flat band shift in the C−V curve is not obvious. Further efforts should be made to improve the film properties before it can be applied as a dielectric.

(25) Zhang, R.; Gao, L. *Key Eng. Mater.* **2002**, *224*−*226*, 573.
(26) (a) Yoko, T.; Kamiya, K.; Tanaka, K. *J. Mater. Sci.* **1990**, *25*, 3922. (b) Zhang, J.; Boyd, I.; O'Sullivan, B. J.; Hurley, P. K.; Kelly, P. V.; Senateur, J.-P. *J. Non-Cryst. Solid* **2002**, *303*, 134.
(27) (a) Koumoto, K.; Masuda, Y.; Wang, D. J. *Int. J. Soc. Mater. Eng. Resour.* **2002**, *10*, 49. (b) Wang, D.-J.; Masuda, Y.; Koumoto, K. *Key Eng. Mater.* **2002**, *214*, 163.
(28) Shin, H.; De Guire, M. R.; Heuer, A. H. *J. Appl. Phys.* **1998**, *83*, 3311.

Conclusions

We reported a novel solution system for site-selective deposition and micropatterning of TiO_2 thin films onto the self-assembled monolayers by the peroxotitanate-complex deposition (PCD) method. This method enables direct preparation of amorphous TiO_2 micropatterns in an aqueous peroxotitanate solution at room temperature. The selectivity, film morphology, thickness, fundamental dielectric properties, and growth mechanism were investigated. The results suggested that the present method is a promising alternative for site-selective deposition of TiO_2 thin films through a low-temperature, environmentally friendly process.

CM030543I